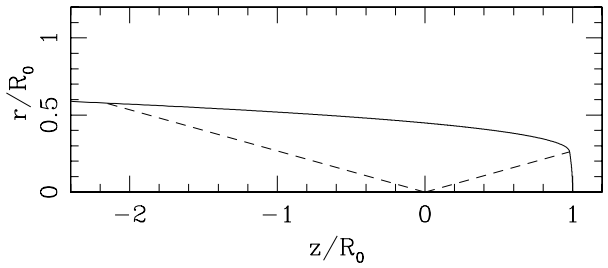

Fig. 2. Analytic solution for the shape of the bow shock produced by the interaction of a bi-conical outflow with an aligned, streaming environment. The outflow cones have a half-opening angle $\theta_j = 15°$, and their outer boundaries are shown by the dashed lines.

$$\times\sqrt{3\,[1+(\pi-\theta-2\theta_j+\sin 2\theta_j)\,\mathrm{cotan}\,\theta]}\,;$$

$$\pi-\theta_j\le\theta\le\pi\,, \tag{9}$$

where

$$R_0\equiv\sqrt{\frac{\dot{M}_j v_j}{2\pi(1-\cos\theta_j)\rho_a v_a^2}}\,, \tag{10}$$

is the on-axis standoff distance between the bow shock and the jet source.

As an example, in Figure 2 we show the bow shock shape obtained from equations (7–9) for a bi-conical outflow with a half-opening angle $\theta_j = 15°$. The solution is quite flat-topped in the $\theta < \theta_j$ "head" region. For $\theta > \theta_j$ the solution first rapidly curves, and then straightens out into a slowly expanding bow shock wing.

3. THE NUMERICAL SIMULATIONS

We have computed seven different axisymmetric gasdynamic simulations of aligned bi-conical jet/streaming environment interactions with the WALICXE code, which is described in detail by Esquivel et al. (2010). The code integrates the gasdynamic equations with an approximate Riemann solver (in this case we used a hybrid HLL-HLLC algorithm, see Harten, Lax, & van Leer 1983; Toro, Spruce, & Speares 1994; Esquivel et al. 2010). A hydrogen ionization rate equation is solved along with the gasdynamic equations in order to include the radiative losses through a parametrized cooling function, that depends on the density, temperature and hydrogen ionization fraction (Raga & Reipurth 2004).

The WALICXE code has a block based adaptive grid, with blocks of a constant number of cells (in our case, of 24×24 cells), which are refined by successive factors of 2. Most of our simulations were run at a medium resolution (labeled "mr" in Table 1). These consist of two root blocks aligned in the axial direction, which are allowed to have 8 levels of refinement. The resolution at the finest level would correspond to 6144×3072 cells (axial and radial, respectively) in a uniform grid. In addition, we ran low and high resolution versions of model 1 (labeled "lr" and "hr" in Table 1). The low resolution run has 7 levels of refinement (3072×1536 cells in a uniform grid), while the high resolution run has 9 levels of refinement (12288×6144 cells in a uniform grid).

Models 1–6 have a computational box of the same size, $[2 \times 4]10^{18}$ cm (radial and axial). Therefore the "mr" runs have a maximum resolution of 6.51×10^{14} cm, and the "lr" and "hr" runs have resolutions of 1.30×10^{15} cm and 3.25×10^{14} cm, respectively. In model 7 we were more interested in resolving the structure at the head of the shock than in the long cometary tail. To achieve a higher resolution (6.51×10^{13} cm) with the same number of computational cells, in these models we have reduced the size of the computational box by a factor of 10.

The simulations were performed in a cylindrical computational grid with an axial extent $[z_{\rm min}, z_{\rm max}]$ (with the jet source placed at $z = 0$) and extending radially from the symmetry axis ($r = 0$, where a reflecting boundary condition is applied) out to $r_{\rm max}$. An inflow condition is applied in the positive z grid boundary, where a streaming environment is injected with a constant velocity in the $-z$ direction. Outflow boundaries were applied at the negative z grid boundary and at $r_{\rm max}$. In models 1–3 $z_{\rm min} = -2.8 \times 10^{18}$ cm and $z_{\rm max} = 1.2 \times 10^{18}$ cm, in models 4–6 $z_{\rm min} = -2.0 \times 10^{18}$ cm and $z_{\rm max} = 2.0 \times 10^{18}$ cm, in model 7 $z_{\rm min} = -2.8 \times 10^{17}$ cm and $z_{\rm max} = 1.2 \times 10^{17}$ cm.

The parameters of the simulations are summarized in Table 1. The jets are imposed in two cones with a half-opening angle Θ and an initial outer radius equal to $R_j = 10^{16}$ cm for models 1–6, and $R_j = 10^{15}$ cm for model 7. The outflows have a velocity v_j (see Table 1) and a temperature $T_j = 100$ K. The density inside the source follows a $\propto R^{-2}$ profile set by the mass loss rate $\dot{M}_j$. The environment has an initial temperature $T_a = 10^4$ K, a density n_a and a velocity v_a. The values for the parameters of models 1–6 are roughly consistent with the jet of Mira B while model 7 (with a denser streaming environment) was chosen to produce a more radiative interaction region. Both the jet and the environment are initially neutral, except for a seed electron density assumed to come from the presence of singly ionized carbon.